In silico evaluation of twenty-five amino derivatives as potential nitric oxide synthase inhibitors

Regina Cauich-Carrillo[1], Marcela Rosas-Nexticapa[2], Magdalena Alvarez-Ramirez[2], Maria Virginia Mateu-Armad[2], Emilio Aguilar-Sanchez[2] & Lauro Figueroa-Valverde[3]

[1] Universidad Vizcaya de las Americas, Av. Boulevard Bahia, 422, Col. Zona de Granjas, Chetumal Quintana Roo, C.P. 77079, Mexico

[2] Nutrition Laboratory, Faculty of Nutrition, University of Veracruz, Medicos y s/n Odontologos 910210, Unidad del Bosque, Xalapa, Mexico

[3] Laboratory of Pharmaco-Chemistry, Faculty of Chemical Biological Sciences, University Autonomous of Campeche, Av. Agustín Melgar s/n, Col Buenavista C.P. 24039, Campeche, Camp., México

Correspondence: Lauro Figueroa-Valverde, Laboratory of Pharmaco-Chemistry, Faculty of Chemical Biological Sciences, University Autonomous of Campeche, Av. Agustín Melgar s/n, Col Buenavista C.P. 24039, Campeche, Camp., México. E-mail: lfiguero@uacam.mx

Received: April 19, 2025 DOI: 10.14295/bjs.v4i8.751

Accepted: June 19, 2025 URL: https://doi.org/10.14295/bjs.v4i8.751

Abstract

There are studies indicating that nitric oxide synthase can be involved in cancer cell growth. It is important to mention that some inhibitors of nitric oxide synthase can produce changes in cancer cell growth. However, there is little information on the interaction of some amino derivatives with nitric oxide synthase surface. The aim of this research was to determine the theoretical interaction of amino derivatives (compounds 1-25) with nitric oxide synthase using the 4d1o protein as a tool. Besides, L-NAME, ONO1714, and N-(3-(aminomethyl)benzyl)acetamidine drugs were used as controls in the DockingServer program. The results showed differences in the number of aminoacid residues and energy levels involved in the interaction of amino derivatives with the 4d1o protein surface compared with the controls. Furthermore, the inhibition constants for amino derivatives 4, 15, 20, 24, and 25 were lower compared to L-NAME and ONO1714 drugs. In conclusion, these theoretical results indicate that compounds 4, 15, 20, 24, and 25 have a higher affinity for the 4d1o protein surface. This data indicates that amino derivatives 4, 15, 20, 24, and 25 can exert changes in the biological activity of nitric oxide synthase. This phenomenon could translate into a decrease in cancer cell growth; however, to validate this hypothesis, it is necessary to perform different experiments in a biological model.

Keywords: amino derivatives, nitric oxide synthase, cancer.

Avaliação *in silico* de vinte e cinco derivados de amino como potenciais inibidores da óxido nítrico sintase

Resumo

Existem estudos que indicam que a óxido nítrico sintase pode estar envolvida no crescimento de células cancerígenas. É importante mencionar que alguns inibidores da óxido nítrico sintase podem produzir alterações no crescimento de células cancerígenas. No entanto, há pouca informação sobre a interação de alguns derivados amino com a superfície da óxido nítrico sintase. O objetivo desta pesquisa foi determinar a interação teórica de derivados amino (compostos 1-25) com a óxido nítrico sintase usando a proteína 4d1o como ferramenta. Além disso, os fármacos L-NAME, ONO1714 e N-(3-(aminometil)benzil)acetamidina foram usados como controles no programa DockingServer. Os resultados mostraram diferenças no número de resíduos de aminoácidos e níveis de energia envolvidos na interação dos derivados amino com a superfície da proteína 4d1o em comparação com os controles. Além disso, as constantes de inibição para os derivados amino 4, 15, 20, 24 e 25 foram menores em comparação aos fármacos L-NAME e ONO1714. Em conclusão, estes resultados teóricos indicam que os compostos 4, 15, 20, 24 e 25 apresentam maior afinidade pela superfície da proteína 4d1o. Esses dados indicam

que os derivados amino 4, 15, 20, 24 e 25 podem exercer alterações na atividade biológica da óxido nítrico sintase. Este fenômeno pode se traduzir em uma diminuição no crescimento de células cancerígenas; no entanto, para validar essa hipótese, é necessário realizar diferentes experimentos em um modelo biológico.

Palavras-chave: derivados de amino, óxido nítrico sintase, câncer.

1. Introduction

Epidemiological data indicate that cancer has increased worldwide, resulting in a decreased population's quality of life (Xia et al., 2022; Siegel et al., 2022; Saad et al., 2022; Lazarus et al., 2022). It is important to mention that several risk factors are involved in the development of cancer, such as alcohol (Yoo et al., 2022; Im et al., 2022), obesity (Aminian et al., 2022), cigarette smoking (Hecht et al., 2022; Phua et al., 2022), dietary fatty acid patterns (Wan et al., 2022; Tu et al., 2022), and some genetic factors (Hauang et al., 2022; Lee et al., 2022). Besides, there are studies indicating that some biomolecules, such as nitric oxide synthase, are involved in changes in cancer cell growth; for example, a study showed that nitric oxide synthase activity was associated with high levels of lung adenocarcinoma (Fujimoto et al., 1997). Another study showed the expression of nitric oxide synthase in breast cancer patients (Loibl et al., 2005). Furthermore, a report indicating that higher nitric oxide levels are related to nitric oxide synthase activity in patients with primary lung cancer (Liu et al., 1998). Another report suggests that nitric oxide synthase expression in breast carcinoma may be an early event in carcinogenesis (Loibl et al., 2002). In addition, a study displayed the expression of nitric oxide synthase in human colorectal cancers, which may correlate with cancer cell growth (Yagihashi et al., 2000).

On the other hand, in the search of some therapeutic alternatives for treat cancer cells some nitric oxide synthase inhibitors have been used; for example a study showed that L-NAME (Nω-nitro-l-arginine methyl ester) reduced tumor growth by 50% using a MCG 101 model (Calhin et al., 2000). Other data indicate that some nitric oxide synthase antagonists such as 1400W (N-(3-(Aminomethyl)benzyl)acetamidine) and L-NIO (*N*-5-(1-Iminoethyl)-L-ornithine) can inhibit the angiogenesis pathway of colorectal cancer using two colorectal cancer cell lines [HT 29 and HCT 116] (Gao et al., 2009). Another report displayed that diprenorphine may decrease nitric oxide synthase activity in T47D human breast cancer cells (Kampa et al., 2001). All results data indicate that nitric oxide synthase inhibitors can modulate cancer cell growth; however, their interaction is highly unclear; this phenomenon may be due to differences in the chemical structure of compounds involved in this process. It is noteworthy that some of these compounds have amino groups in their chemical structure, which could result in changes in the biological activity of nitric oxide synthase. Analyzing these data, the objective of this investigation was to evaluate the interaction of twenty five amino-derivatives with nitric oxide synthase enzyme using 4d1o protein as theoretical tool in DockingServer.

2. Materials and Methods

Twenty-five amino derivatives (Figure 1) were used to evaluate their possible interaction with both nitric oxide synthase as follows:

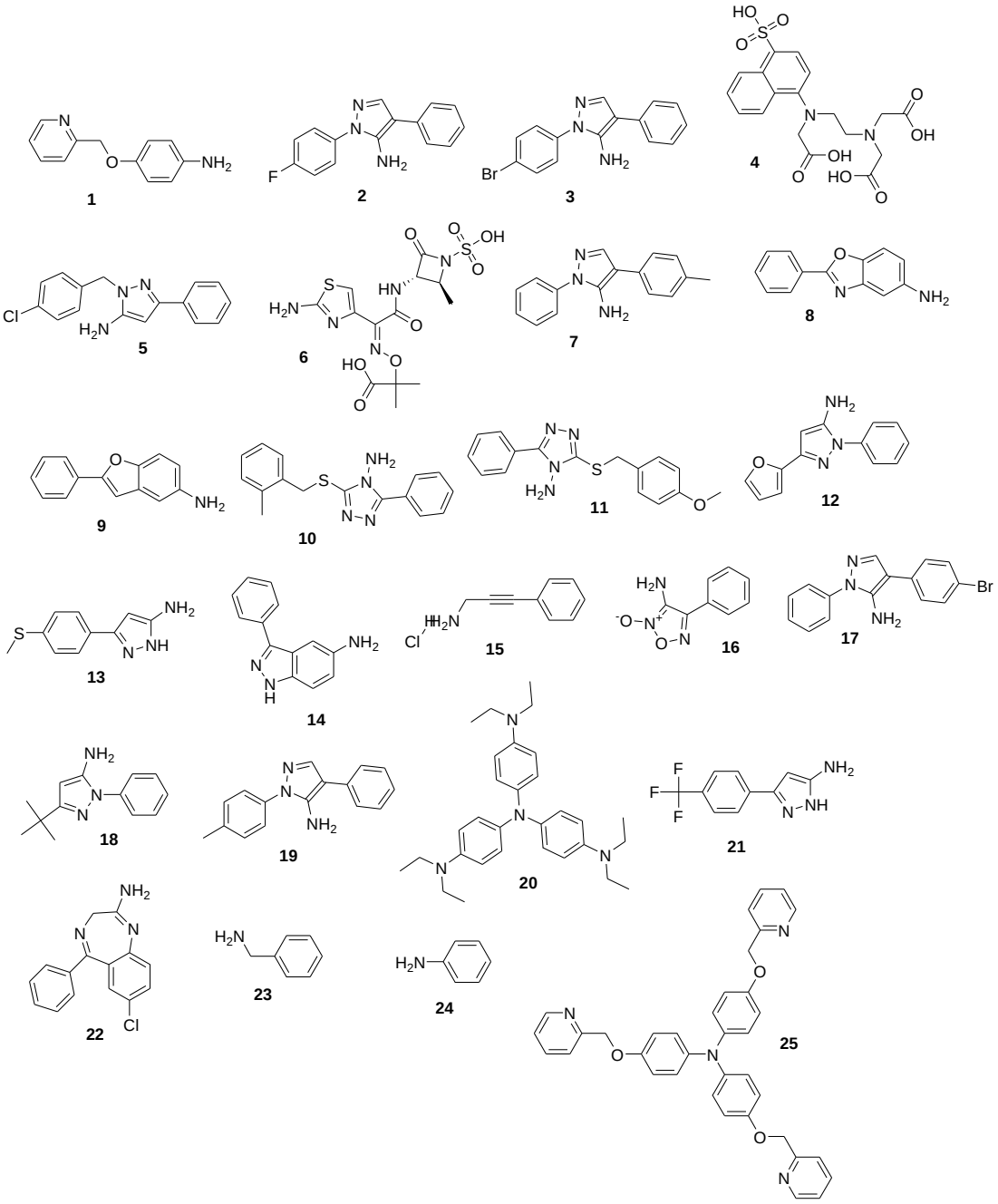

Figure 1. Chemical structure of amino derivatives (**1**-**25**). Source: https://pubchem.ncbi.nlm.nih.gov/.

Table 1. Chemical names of amino derivatives.

1	4-(2-pyridylmethoxy)aniline
2	2-(4-fluorophenyl)-4-phenyl-pyrazol-3-amine
3	2-(4-bromophenyl)-4-phenyl-pyrazol-3-amine
4	2-[carboxymethyl-[2-[carboxymethyl-(4-sulfo-1-naphthyl)amino]ethyl]amino]acetic acid
5	2-[(4-chlorophenyl)methyl]-5-phenyl-pyrazol-3-amine
6	2-[(*Z*)-[1-(2-aminothiazol-4-yl)-2-[[(2*S*,3*S*)-2-methyl-4-oxo-1-sulfo-azetidin-3-yl]amino]-2-oxo-ethylidene] amino]oxy-2-methyl-propanoic acid
7	2-phenyl-4-(p-tolyl)pyrazol-3-amine
8	2-phenyl-1,3-benzoxazol-5-amine
9	2-phenylbenzofuran-5-amine
10	3-(o-tolylmethylsulfanyl)-5-phenyl-1,2,4-triazol-4-amine
11	3-[(4-methoxyphenyl)methylsulfanyl]-5-phenyl-1,2,4-triazol-4-amine
12	5-(2-furyl)-2-phenyl-pyrazol-3-amine
13	3-(4-methylsulfanylphenyl)-1*H*-pyrazol-5-amine
14	3-phenyl-1*H*-indazol-5-amine
15	3-phenylprop-2-yn-1-amine;hydrochloride
16	2-oxido-4-phenyl-1,2,5-oxadiazol-2-ium-3-amine
17	4-(4-bromophenyl)-2-phenyl-pyrazol-3-amine
18	5-*tert*-butyl-2-phenyl-pyrazol-3-amine
19	4-phenyl-2-(p-tolyl)pyrazol-3-amine
20	*N*1,*N*1-bis[4-(diethylamino)phenyl]-*N*4,*N*4-diethyl-benzene-1,4-diamine
21	3-[4-(trifluoromethyl)phenyl]-1*H*-pyrazol-5-amine
22	7-chloro-5-phenyl-3*H*-1,4-benzodiazepin-2-amine
23	phenylmethanamine
24	phenylamine.
25	4-(2-pyridylmethoxy)-*N*,*N*-bis[4-(2-pyridylmethoxy)phenyl]aniline

2.1 Pharmacophore model

3D pharmacophore model for amino derivatives (**1** to **25**) was evaluated using LigandScout 4.08 software (Chiarelly et al., 2018). LigandScout is a program that allows you to create three-dimensional (3D) models of pharmacophores from different compounds to characterize some their chemical properties such as hydrogen bond donors, acceptors, lipophilic areas and positively and negatively ionizable chemical groups that can be used to predict interactions of different drugs with some biomolecules.

2.2 Ligand-Protein analysis

The coupling of amino-derivatives with 4d1o protein surface was determined with DockingServer program (Bikadi, Hazai, 2009, Kong et al., 2020). It is important to mention that this program involve the MMFF94 force field (Halgren, 1998) which is used for energy minimization of ligand molecule (amino derivatives) using DockingServer. Gasteiger partial charges were added to the ligand atoms. Non-polar hydrogen atoms were merged, and rotatable bonds were defined. Besides, docking calculations were carried out on 4d1o protein model. It is noteworthy that essential hydrogen atoms, Kollman united atom type charges, and solvation parameters were added with the aid of AutoDock tools (Morris, Goodsell et al., 1998). Affinity (grid) maps of 20×20×20 Å grid points and 0.375 Å spacing were generated using the Autogrid program (Morris, Goodsell et al., 1998). In addition, AutoDock parameter set- and distance-dependent dielectric functions were used in the calculation of

the van der Waals and the electrostatic terms, respectively. Also, docking simulations were performed using the Lamarckian genetic algorithm (LGA) and the Solis & Wets local search method (Solis and Wets, 1981). Initial position, orientation, and torsions of the ligand molecules were set randomly. Each docking experiment was derived from 2 different runs that were set to terminate after a maximum of 250000 energy evaluations. The population size was set to 150. During the search, a translational step of 0.2 Å, and quaternion and torsion steps of 5 were applied. Besides, two nitric oxide synthase inhibitors such as ONO1714 (7-Chloro-5-methyl-2-aza-bicyclo[4.1.0]hept-2-en-3-ylamine; hydrochloride), and N-(3-(Aminomethyl)-benzyl)acetamidine (Minhas et al., 2020) were used as controls.

2.3 Pharmacokinetics parameter

Pharmacokinetic factors for amino derivatives 5, 15, 20, 24, and 25 were determined using the Swiss ADME software [http://www.swissadme.ch/index.php] Bakchi et al., 2022).

2.4 Toxicology analysis

Toxicology evaluation for amino derivatives 5, 15, 20, 24, and 25 were determined using the Gussar software [https://www.way2drug.com/Gusar/acutoxpredict.html] (Khrapova et al., 2023).

3. Results

Pharmacophore models for amino derivatives (1-25) are showed in Figures 2-5 using LigandScout 4.0 program. The results indicate showed different type of hydrogen bond donors and acceptors, lipophilic areas and positively and negatively ionizable chemical groups for different steroid derivatives.

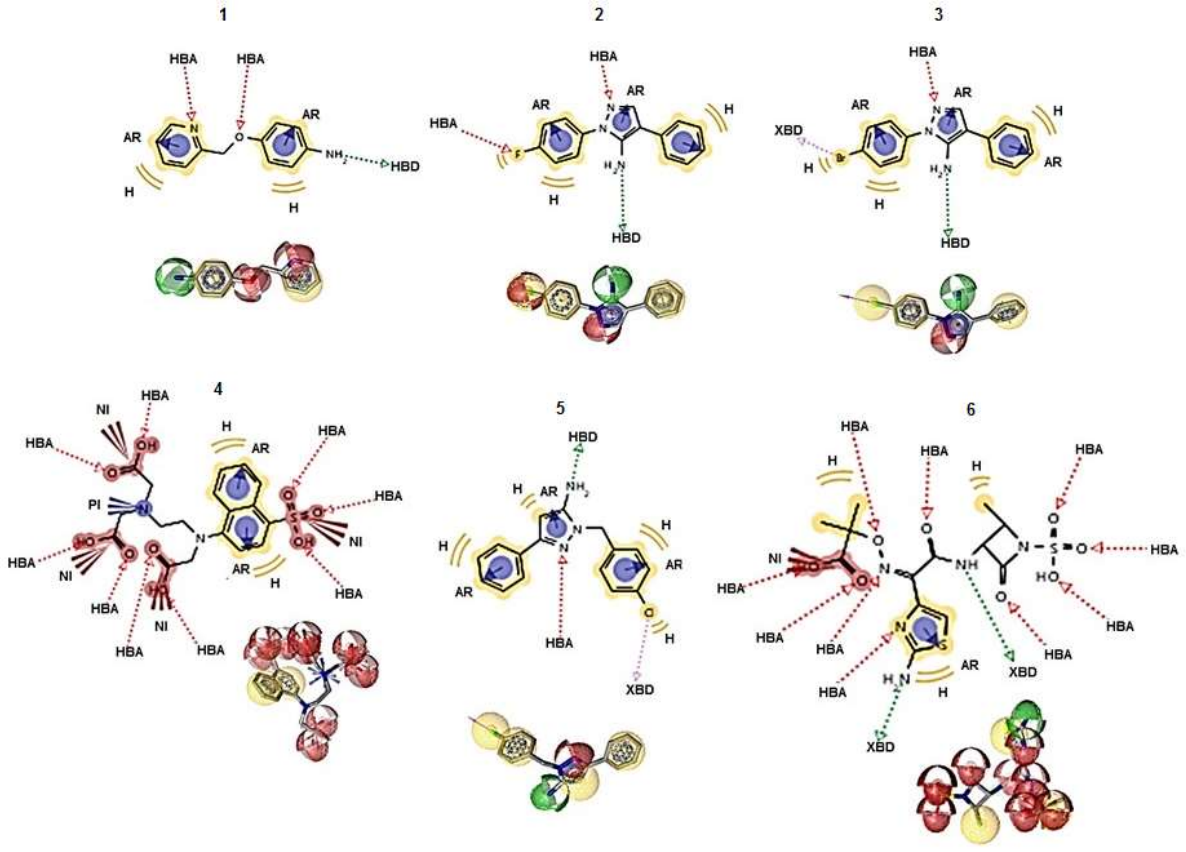

Figure 1. Pharmacophore models from amino-derivatives (1 to 8). Visualized with LigandScout program. Hydrogen bond acceptors (HBA, red), and hydrogen bond donors (HBD, green).

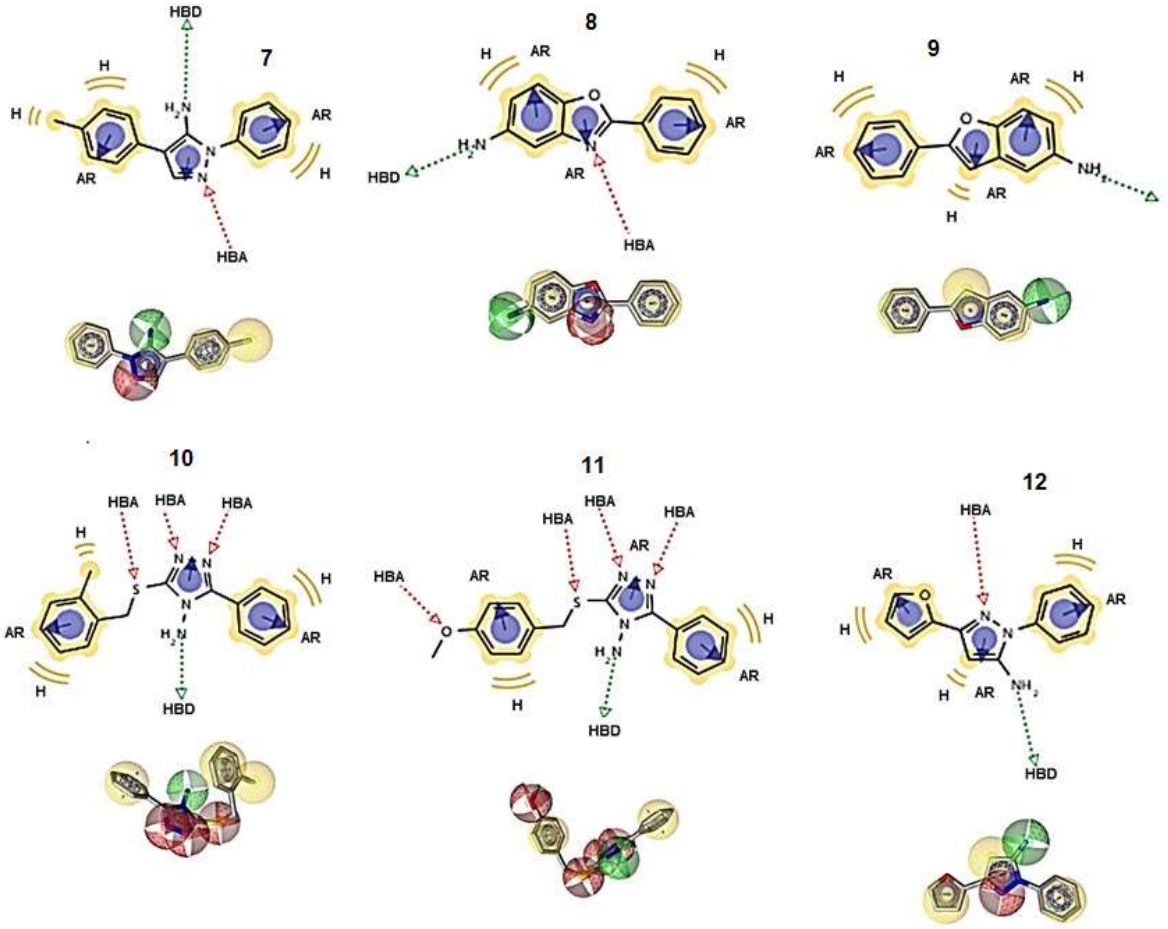

Figure 2. The scheme shows pharmacophore models for amino derivatives (9 to 16). Visualized with LigandScout software. Hydrogen bond acceptors (HBA, red), and hydrogen bond donors (HBD, green).

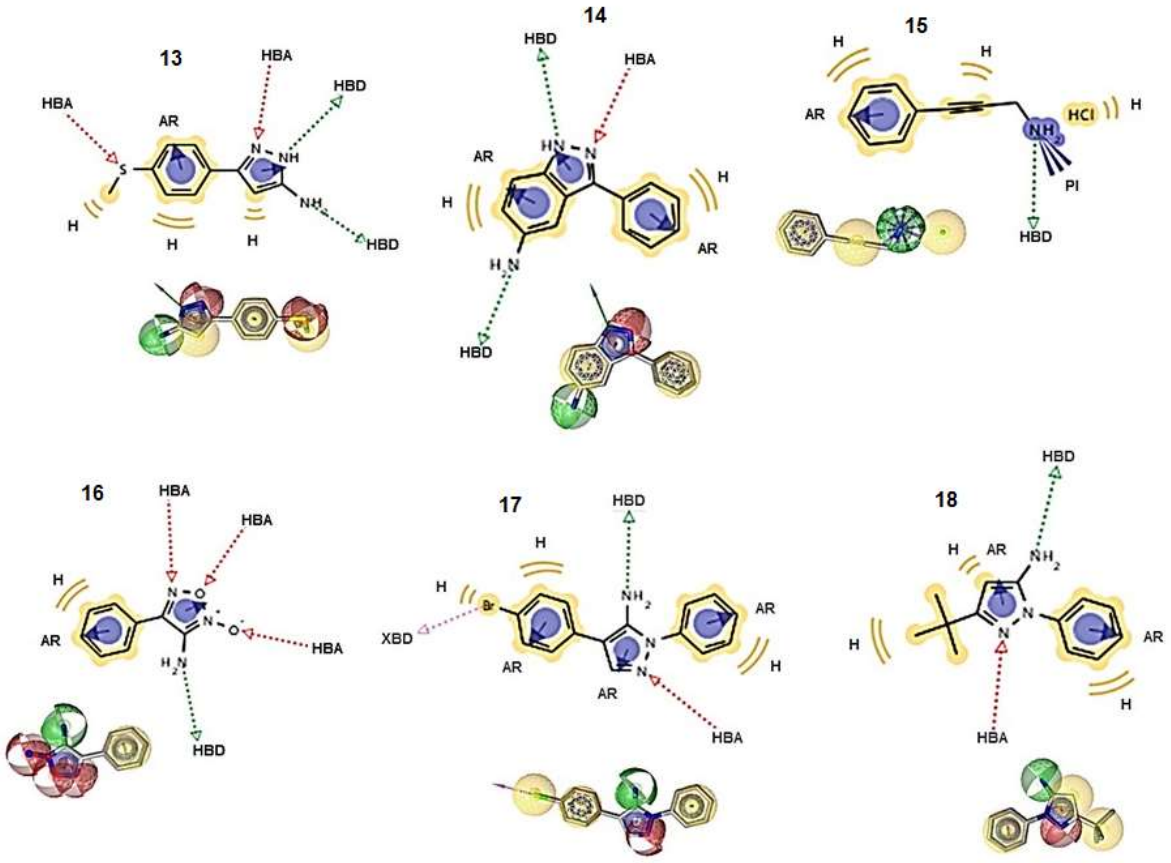

Figure 3. Pharmacophore model for compounds 13 to 18. Visualized with LigandScout program. Hydrogen bond acceptors (HBA, red), and hydrogen bond donors (HBD, green).

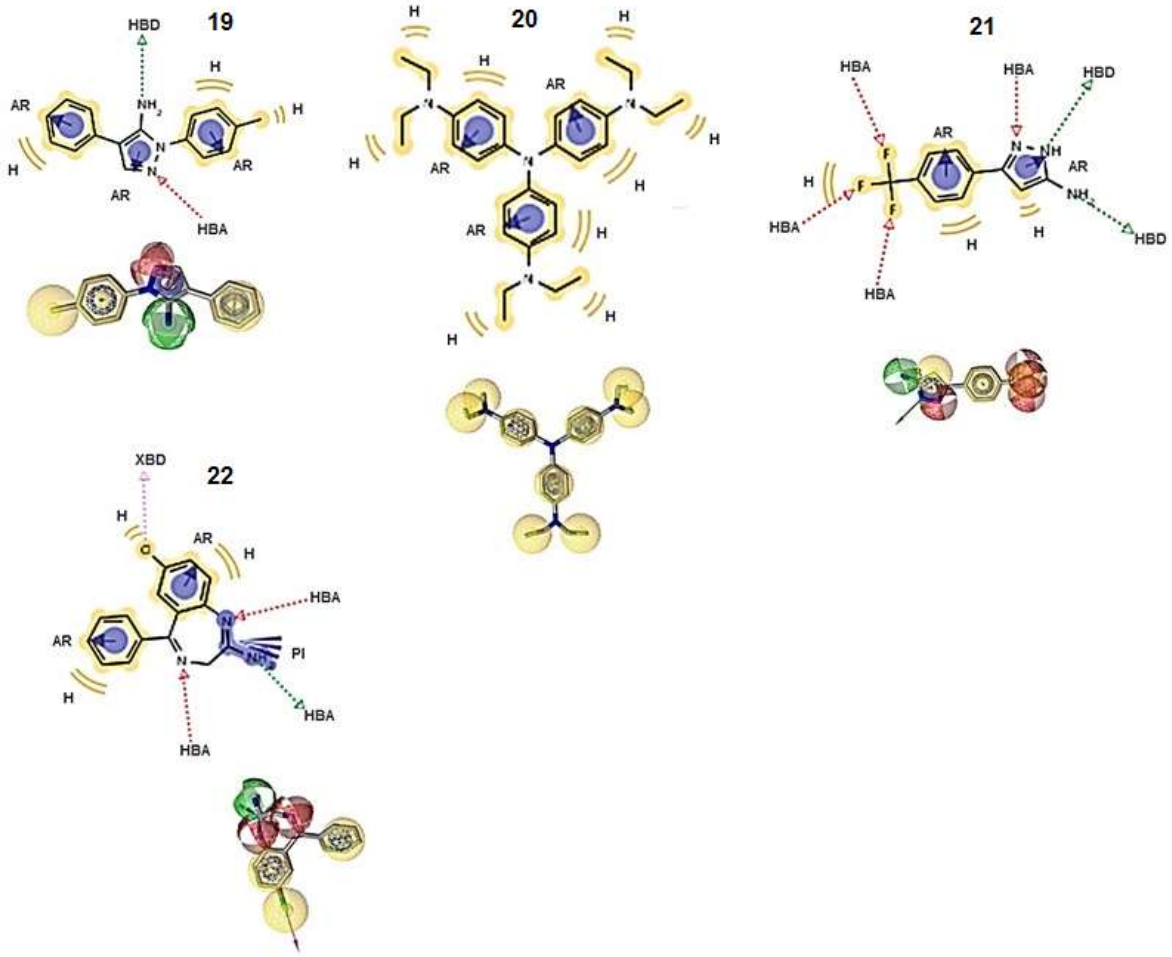

Figure 4. The scheme shows pharmacophore models for compounds (19 to 22). Visualized with LigandScout program. Hydrogen bond acceptors (HBA, red), and hydrogen bond donors (HBD, green).

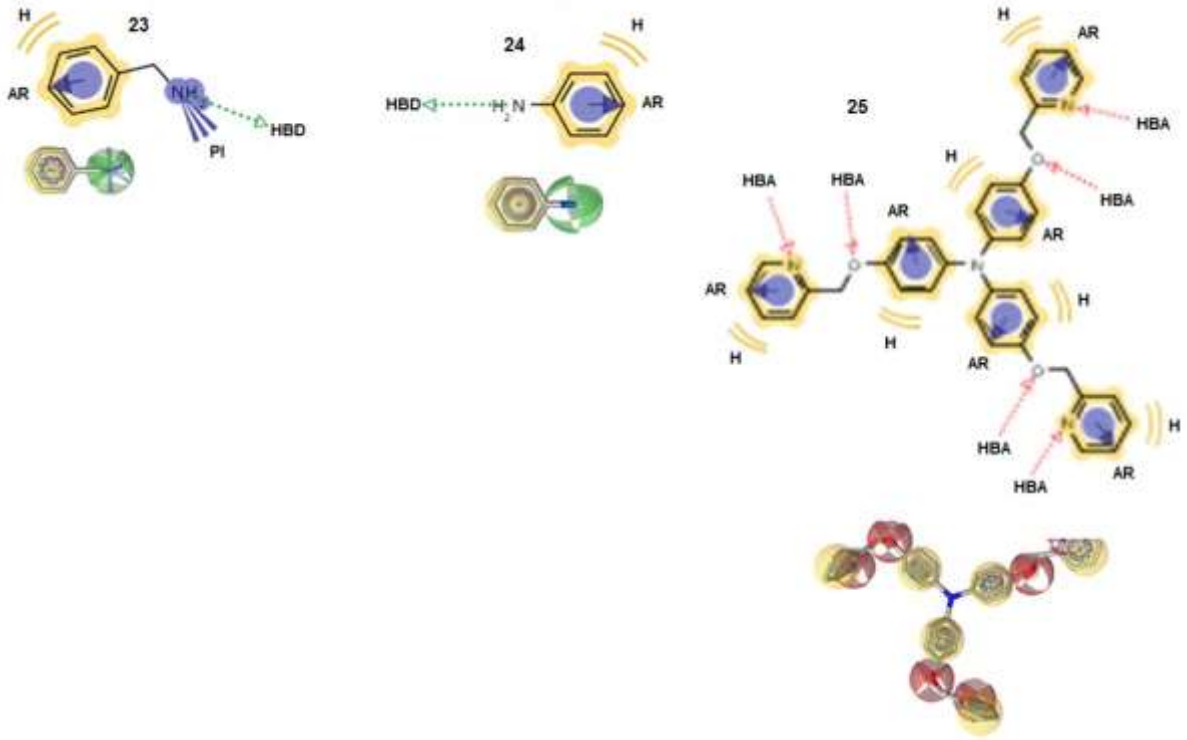

Figure 5. The scheme shown the pharmacophores from compounds 23 to 25. Visualized with LigandScout program. Hydrogen bond acceptors (HBA, red), and hydrogen bond donors (HBD, green).

3.1 Ligand-Protein

The results of interaction from amino-derivatives (1-25) and the controls (L-NAME, ONO1714, and N-(3-(aminomethyl)benzyl)acetamidine) with 4dlo protein surface are showed in the Table 2.

Table 2. Coupling of amino-derivative (1-25), L-NAME (I), ONO1714 (II), and N-(3-(aminomethyl)benzyl)acetamidine (III) with 4d1o protein surface.

Compound	Aminoacid Residues
I	Gln_{411}; $Thr_{416;}$ Ile_{417}; Val_{418}; Asp_{419}; Ala_{422}
II	Val_{185}; $Met_{358;}$ Thr_{360}; Gln_{361}; $Arg_{365;}$ Trp_{447}; $Val_{449;}$ Pro_{451}
II	Gln_{411}; Ile_{417}; Val_{418}; Asp_{419}; Ala_{422}
1	$Val_{185;}$; Ile_{188}; Gln_{189}; Trp_{356}; $Thr_{416;}$ Val_{418}; Ala_{423}; Ser_{426}
2	Ile_{188}; Trp_{356}; Gln_{411}; $Thr_{416;}$ Ile_{417}; $Val_{418;}$ Ser_{426}
3	Ile_{188}; Gln_{189}; Trp_{356}; $Thr_{416;}$ Val_{418}; Ser_{426}; Lys_{429}
4	Ile_{188}; Gln_{189}; $Lys_{192;}$ Asn_{223}; Trp_{356}; $Thr_{416;}$ Ser_{426}
5	Gln_{189}; Lys_{192}; Asn_{223}; Leu_{224}; Trp_{356}; $Val_{418;}$ Ala_{423}; Ser_{426}
6	Val_{185}; Ile_{188}; Gln_{189}; $Lys_{192;}$ Trp_{356}; Ala_{423}; Ser_{426}
7	Ile_{188}; Gln_{189}; Trp_{356}; $Thr_{416;}$ Val_{418}; Ala_{423}; Ser_{426}
8	Val_{185}; $_{;}$ Ile_{188}; Gln_{189}; Trp_{356}; Thr_{416} ; $Val_{418;}$ Ala_{423}; Ser_{426}
9	Gln_{189}; Asn_{223}; Leu_{224}; Trp_{356}; $Thr_{416;}$ Val_{418}
10	Gln_{189}; Trp_{356}; $Thr_{416;}$ Ile_{417}; $Val_{418;}$ Ala_{423}; Ser_{426}
11	Ile_{188}; Gln_{189}; $Val_{418;}$ Ala_{423}; Ala_{424}; $Ser_{426;}$ Lys_{429}
12	Ile_{188}; Gln_{189}; Trp_{356}; $Thr_{416;}$ Val_{418}; Ala_{423}; Ser_{426}
13	Val_{185}; Gly_{186}; Ile_{188}; Gln_{189}; Trp_{356}; $Thr_{416;}$ Val_{418}; Ala_{423}; Ser_{426}
14	Ile_{188}; Gln_{189}; Trp_{356}; Ile_{417}; $Val_{418;}$ Ala_{423}; Ser_{426}
15	Ile_{188}; Gln_{189}; $Trp_{356;}$ $Thr_{416;}$ Ile_{417}; $Val_{418;}$ Ala_{423}; Ser_{426}
16	Gln_{189}; $Lys_{192;}$ Typ_{217}; $Leu_{224;}$ Arg_{225}; $Ser_{226;}$ Trp_{356}
17	Gln_{189}; Trp_{356}; $Val_{418;}$ Ala_{422}; Ala_{423}; Ser_{426}
18	Gln_{189}; Trp_{356}; $Thr_{416;}$ $Val_{418;}$ Ala_{423}; Ser_{426}
19	Ile_{188}; Gln_{189}; $Trp_{356;}$ $Thr_{416;}$ $_{;}$ Val_{418}; $Ser_{426;}$ Lys_{429}
20	Ile_{188}; Gln_{189}; $Trp_{356;}$ $Thr_{416;}$ $_{;}$ Val_{418}; Ala_{422}; Ala_{425}; Ser_{426}
21	Gln_{189}; $Lys_{192;}$ Trp_{356}; $Thr_{416;}$ Ile_{417}; Val_{418}
22	Ile_{188}; Gln_{189}; $Trp_{356;}$ $Thr_{416;}$ $_{;}$ Ile_{417}; Val_{418}; Ala_{422}; Ala_{425}; Ser_{426}
23	Val_{185}; Met_{358}; Gln_{361}; $Arg_{365;}$ Pro_{450}; Pro_{451}
24	Val_{185}; Gln_{189}; $Trp_{356;}$ Val_{418}; Ala_{425} Ser_{426}
25	Gln_{189}; $Lys_{192;}$ Asn_{223}; Trp_{356}; Gln_{411}; $Thr_{416;}$ Val_{418}; Asp_{419}; Ala_{422}

On the other hand, Table 3 displays the energies values and inhibition constant (Ki) involved in the coupling of amino-derivatives (1-25), ONO1714, and N-(3-(aminomethyl)benzyl)acetamidine with 4dlo protein surface. Its is noteworthy that inhibition constants (Table 4) for compound 4, 15, 20, 24, and 25 was lower compared with L-NAME (I), ONO1714 (II), and N-(3-(aminomethyl)benzyl)acetamidine (III)

Table 3. Thermodynamic parameters involved in the interaction of amino derivatives (1-25), L-NAME (I), ONO1714 (II), and N-(3-(aminomethyl)benzyl)acetamidine (III) with 4d1o protein surface.

Compound	**A**	**B**	**C**	**D**	**E**	**F**
I	-4.29	714.67	-2.99	-1.59	-4.58	375.78
II	-6.17	29.80	-5.27	-0.90	-6.17	420.41
III	-3.25	4.11	-3.32	-1.42	-4.74	401.54
1	-4.60	427.84	-5.57	-0.07	-5.64	450.447
2	-4.82	295.19	-5.74	-0.06	-5.81	520.114
3	-4.15	902.84	-4.99	-0.06	-5.05	487.345
4	-3.05	5.80	-5.38	-0.61	-5.98	644.607
5	-5.03	203.91	-6.19	-0.00	-6.19	587.667
6	-4.78	311.20	-5.35	-0.96	-6.31	567.055
7	-4.34	658.57	-5.22	-0.02	-5.24	487.273
8	-4.47	525.52	-5.00	-0.07	-5.07	431.492
9	-4.25	760.80	-4.79	-0.06	-4.85	528.929
10	-5.30	130.59	-6.51	-0.00	-6.51	561.682
11	-4.47	531.22	-5.96	-0.09	-6.05	538.509
12	-4.40	595.75	-5.25	-0.04	-5.29	483.122
13	-4.53	475.71	-5.35	-0.09	-5.43	442.65
14	-5.26	138.51	-5.83	-0.04	-5.87	445.242
15	-3.94	1.29	-4.61	-0.22	-4.84	396.339
16	-4.94	239.74	-5.43	+0.19	-5.24	431.046
17	-4.10	984.64	-5.07	-0.04	-5.11	426.898
18	-4.66	382.59	-5.54	-0.01	-5.56	485.26
19	-4.12	951.54	-4.97	-0.05	-5.02	514.986
20	-2.75	9.68	-5.72	-0.00	-5.72	815.56
21	-4.39	600.95	-5.08	-0.22	-5.29	418.971
22	-6.08	34.84	-6.55	-0.14	-6.69	523.52
23	-4.37	624.91	-3,81	-1.16	-4.97	330.26
24	-3.98	1.21	-4.22	-0.06	-4.28	291.20
25	-3.30	3.84	-5.06	-0.07	-5.13	770.08

A = Est: Free Energy of Binding (kcal/mol); **B** = Inhibition Constant, Ki (mM); **C** = vdW + Hbond + desolv Energy (kcal/mol); **D** = Electrostatic Energy (kcal/mol); **E** = Total Intermolec. Energy (kcal/mol); **F** = Interact. Surface.

Table 4. Energy levels and the inhibition constants values for compounds 4, 15, 20, 24, and 25.

Compound	**A**	**B**	**C**	**D**	**E**	**F**
4	-3.05	5.80	-5.38	-0.61	-5.98	644.607
15	-3.94	1.29	-4.61	-0.22	-4.84	396.339
20	-2.75	9.68	-5.72	-0.00	-5.72	815.56
24	-3.98	1.21	-4.22	-0.06	-4.28	291.20
25	-3.30	3.84	-5.06	-0.07	-5.13	770.08

A = Est: Free Energy of Binding (kcal/mol); **B** = Inhibition Constant, Ki (mM); **C** = vdW + Hbond + desolv Energy (kcal/mol); **D** = Electrostatic Energy (kcal/mol); **E** = Total Intermolec. Energy (kcal/mol); **F** = Interact. Surface.

On the other hand, Table 5 and Figure 6 show the interactions involved in the formation of the ligand-protein complex. The results indicate that $Trp_{356\ is}$ specific for interaction of amino-derivatives 4, 15, 20, 24, and 25 through pi-pi bonds.

Table 5. Aminocid residues involved in the interation of amino-derivatives (4, 15, 20, 24, and 25) with 4d1o protein surface.

Compounds	**Interaction bonds**				
	Hydrogen	Polar	Hydrophobic	pi-pi	cation-pi
4	Lys_{192}; Thr_{416}	Gln_{189}; Asn_{223}	Ile_{188}; Trp_{356}	Trp_{356}	Trp_{356}
15	Ile_{417}; Trp_{356}; Trp_{416}; Val_{418}		Ile_{188}; Trp_{356}; Val_{418}	Trp_{356}	
20			Ile_{188}; Trp_{356}; Val_{418}; Ala_{422}; Ala_{425}	Trp_{356}	
24	Val_{185}; Ala_{423}; Ser_{426}		Val_{418}; Ala_{423}	Trp_{356}	
25	Gln_{189}	Val_{418}; Ala_{422}		Trp_{356}	

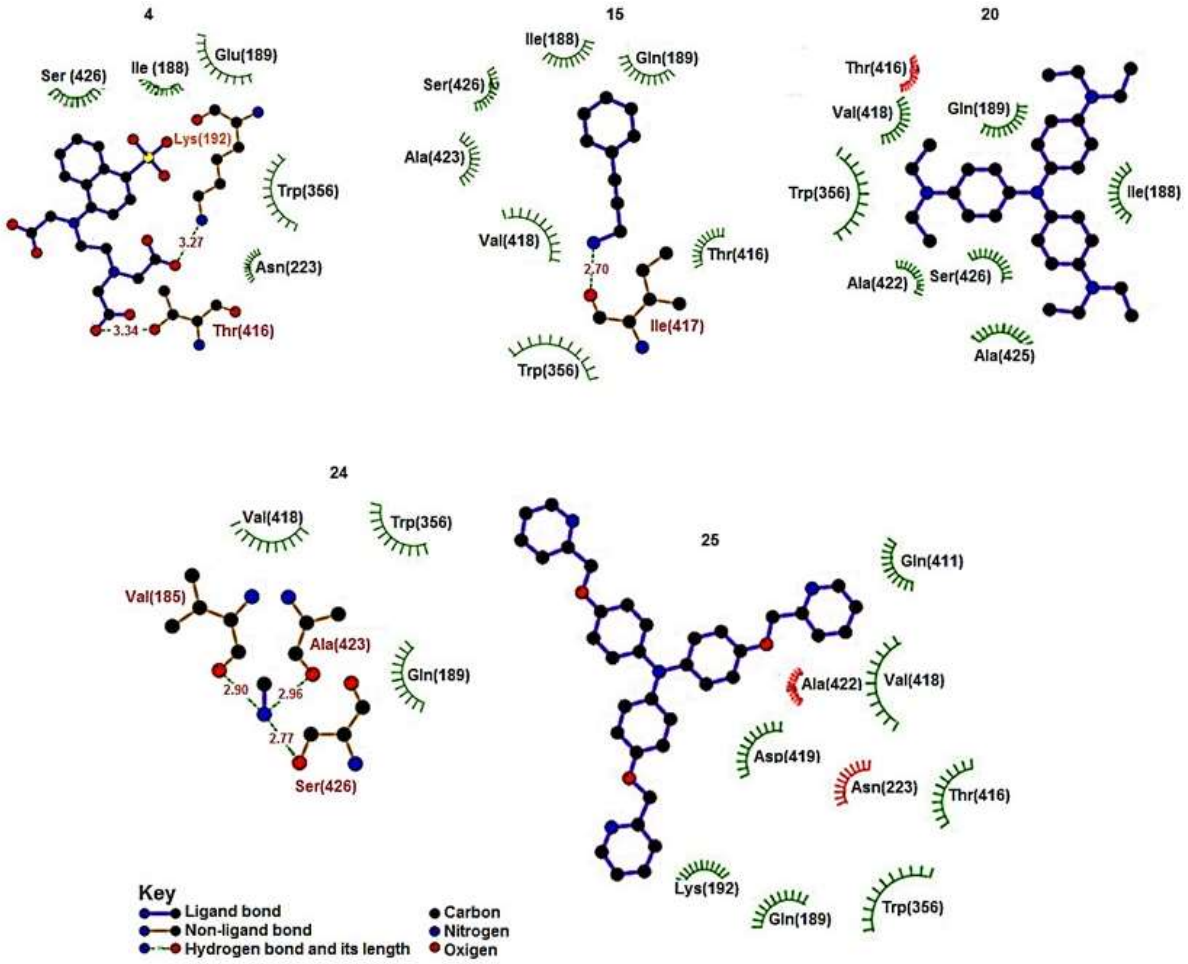

Figure 6. Interaction of amino-derivatives (4, 15, 20, 24, and 25) with 4d1o protein surface. Visualizzed with DockingServer program.

3.2 Pharmacokinetics parameter

The pharmacokinetic values for amino-derivatives 4, 15, 20, 24, and 25 are shown in the Table 6 using SwissADME.

Table 6. Pharmacokinetic parameters for amino derivatives (4, 15, 20, 24, and 25), L-NAME (I), ONO1714 (II), and N-(3-(aminomethyl)benzyl)acetamidine (III).

Parameters	Amino-derivatives							
	I	**II**	**III**	**4**	**15**	**20**	**24**	**25**
GI absorption	Low	High	High	Low	High	Low	High	Low
BBB permeant	No	Yes	Yes	No	Yes	No	Yes	No
P-gp sustrate	No	No	No	No	No	Yes	No	No
CYP1A2 inhibitor	No	No	No	Yes	No	Yes	Yes	No
CYP2C19 inhibitor	No	No	No	No	No	No	No	Yes
CYP2C9 inhibitor	No	No	No	No	No	No	No	No
CYP2D6 inhibitor	No	No	No	No	No	No	No	No
CYP3A4 inhibitor	No	No	No	No	No	No	No	Yes
Consensus $LogP_{O/W}$	-1.32	1.18	1.06	-0.10	1.61	6.35	1.22	5.72

Finally, the possible toxicology degree is showed in the table 7.

Table 7. Toxicology analysis for amino derivatives (5, 15, 20, 24, and 25), L-NAME (I), ONO1714 (II), and N-(3-(aminomethyl)benzyl)acetamidine (III).

Compound	IP LD50 (mg/kg)	IV LD50 (mg/kg)	Oral LD50 (mg/kg)	SC LD50 (mg/kg)
I	253.30	271.20	1589.00	606.30
II	224.10	70.40	430.90	105.00
III	140.20	69.32	570.30	333.70
4	930.10	710.90	4573.00	939.20
15	265.40	30.90	1046.00	397.20
20	305.60	61.76	1490.00	359.90
24	186.50	43.18	397.00	187.20
25	911.30	179.20	1764.00	1777.00

4. Discussion

Theoretical models have been proposed to characterize the interaction of various drugs with different biomolecules. For example, three-dimensional pharmacophore models have been developed, which involve aspects of the chemical structure of some compounds for their possible interaction with some biomolecules (Yang, 2010; Qing et al., 2014; Scholler et al., 2020). In this way, the LigandScout program, which is used for the development of pharmacophores based on chemical structures involving interactions between ligands and macromolecules (Wolber and Langer, 2005; Wolber and Kosara, 2006; Lohachova et al., 2024; Figueroa-Valverde et al., 2024). For this reason, in this study the LigandScout program was used to characterize the functional groups involved in the chemical structure of amino derivatives that could interact with some biomolecules. Figures 2 to 5 displayed pharmacophores for amino derivatives (1-25), which displayed different functional groups that may act as hydrogen bond acceptors (HBA), hydrogen bond donors (HBD), and halogen bond donors (XBD). It is important to mention that this phenomenon could condition their interaction with some biomolecules.

4.1 Ligand-protein complex

There are several theoretical methods used to characterize the ligand-protein formation, such as SwissDOCK (Bugnon et al., 2024), GOLD (Verdonk et al., 2003), GROMAS (Krishnamoorthy et al., 2023), and DockingServer (Hazai et al., 2009). Analyzing these data, the aim of this study was to determine the interaction of amino derivatives with nitric oxide synthase surface using the 4d1o protein as a theoretical tool. Besides, some

nitric oxide synthase inhibitors such as L-NAME (Swan et al., 2024), ONO1714 (7-Chloro-5-methyl-2-aza-bicyclo[4.1.0]hept-2-en-3-ylamine; hydrochloride), and N-(3-(Aminomethyl)-benzyl)acetamidine (Minhas et al., 2020) were used as controls in the DockingServer program. Theoretical data showed different amino acid residues involved in the interaction of amino derivatives with the 4d1o protein surface compared to ONO1714 and -(3-(aminomethyl)benzyl)acetamidine compounds; this phenomenon could be due to differences in the chemical structure of each amino derivative. Besides, the inhibition constant for amino derivatives (15, 24, and 25) was lower compared to L-NAME, ONO1714, and N-(3-(aminomethyl)benzyl)acetamidine compounds. Other data indicate that Ki for amino derivatives 4 and 20 was lower in comparison with L-NAME and ONO174 drugs; this phenomenon can due to 1) differences in the functional groups involved in the chemical structure of amino derivatives compared with the controls.

On the other hand, it is important to mention that aminoacid residue Trp356 involved in the 4d1o protein surface interact the compounds 4, 15, 20, 24 and 25 through pi-pi bonds. However, it is noteworthy that the Ki for compound 20 was lower compared to compounds 4, 15, 24 and 25; these results suggest that the interaction of compound 20 on the surface of protein 4d1o depends on amino acid residues Ala_{422} and Ala_{425} through hydrophobic bonds which is translated as higher affinity by 4d1o protein surface.

4.2 Pharmacokinetic parameters

Some pharmacokinetic parameters were determined using the SwissADME program. The results display that metabolism of amino derivatives could involve different CYPs (P450 family). Besides, the lipophilicity degree for compounds 15, 20, 24, and 25 was higher compared with the controls. This data suggests that the lipophilicity degree of amino derivatives could condition their biological activity exerted on the nitric oxide synthase enzyme.

4.3 Toxicity evaluation

Several methods have been used to predict the toxicity degree of different drugs, such as ProTox-II (Banerjee et al., 2018), ToxAlert (Sushko et al., 2012), Gussar (Askerova, 2023), and others. In this research, the possible toxicity exerted by amino derivatives 4, 15, 20, 24, and 25 was evaluated using the Gussar program. Theoretical data indicate that the degree of toxicity produced by amino derivatives could depend on the dose administered through different routes of administration. Besides, the dose required for amino-derivative 20 was lower compared with 4, 15, 24, 25, and the controls.

5. Conclusions

In order to characterize the interaction of amino derivatives with nitric oxide synthase, the 4d1o protein was used as a theoretical tool. The results indicate that the affinity of different compounds for the 4d1o protein surface depends on certain chemical parameters, such as the amino groups involved in their chemical structure and steric hindrance (provided by the different functional groups), which are two important factors involved in the protein-ligand formation. These data suggest that aminoacid derivatives 4, 15, 20, 24, and 25 could act as nitric oxide synthase inhibitors, and this phenomenon can translate into changes in cancer cell growth. However, to validate this hypothesis, it is necessary to carry out 1) an evaluation of the activity of different aminoacid derivatives using some biological model and 2) a determination of different physicochemical parameters such as molar refractivity, molar volume, and others involved in the structure-activity of the compounds.

6. Authors' Contributions

Substantial contribution to research design: Regina Cauich-Carrillo and Lauro Figueroa-Valverde. Acquisition, analysis and interpretation of data: Marcela Rosas-Nexticapa, Magdalena Alvarez-Ramirez, Marcela Rosas-Nexticapa, and Virginia Mateu-Armand. Approval of the submitted and final versions: all authors.

7. Conflict of interest

The authors declare that this research has no conflict of interest with any public or private association.

8. Ethics Approval

Not applicable.

9. References

Aminian, A., Wilson, R., Al-Kurd, A., Tu, C., Milinovich, A., & Kroh, M. (2022). Association of bariatric surgery with cancer risk and mortality in adults with obesity. *Journal of American Medical Asocciation*, 327(24), 2423-33. https://doi.org/10.1001/jama.2022.9009

Askerova, U. F. (2023). Prediction of acute toxicity for (Z)-3-(2-phenylhydrazinylidene) benzofuran-2 (3H)-one and its derivatives for rats using GUSAR program. *New Materials, Compounds and Applications*, 7(1), 50-56.

Bakchi, B., Krishna, A. D., Sreecharan, E., Ganesh, V. B. J., Niharika, M., Maharshi, S., & Shaik, A. B. (2022). An overview on applications of SwissADME web tool in the design and development of anticancer, antitubercular and antimicrobial agents: a medicinal chemist's perspective. *Journal of Molecular Structure*, 1259, 132712. https://doi.org/10.1016/j.molstruc.2022.132712

Banerjee, P., Eckert, A. O., Schrey, A. K., & Preissner, R. (2018). ProTox-II: a webserver for the prediction of toxicity of chemicals. *Nucleic acids research*, 46(W1), W257-W263. https://doi.org/10.1093/nar/gky318

Bikadi, Z., Hazai, E. (2009). Application of the PM6 semi-empirical method to modeling proteins enhances docking accuracy of AutoDock. *Journal of Cheminformatics*, 1, 15.

Bugnon, M., Röhrig, U. F., Goullieux, M., Perez, M. A., Daina, A., Michielin, O., & Zoete, V. (2024). SwissDock 2024: major enhancements for small-molecule docking with Attracting Cavities and AutoDock Vina. *Nucleic acids research*, 52(W1), W324-W332. https://doi.org/10.1093/nar/gkae300

Cahlin, C., Gelin, J., Delbro, D., Lönnroth, C., Doi, C., & Lundholm, K. (2000). Effect of cyclooxygenase and nitric oxide synthase inhibitors on tumor growth in mouse tumor models with and without cancer cachexia related to prostanoids. *Cancer Research*, 60(6), 1742-1749.

Chiarelli, L. R., Mori, M., Barlocco, D., Beretta, G., Gelain, A., Pini, E., & Meneghetti, F. (2018). Discovery and development of novel salicylate synthase (MbtI) furanic inhibitors as antitubercular agents. *European Journal of Medicinal Chemistry*, 155, 754-763. https://doi.org/10.1016/j.ejmech.2018.06.033

Figueroa-Valverde, L., Rosas-Nexticapa, M., Alvarez-Ramirez, M., Aguilar-Sanchez, E., Mateu-Armad, M. V., & Bonilla-Zavaleta, E. (2024). Interaction of some chalcone derivatives with calcium channels using a theoretical model. *Brazilian Journal of Science*, 3(11), 1-15. https://doi.org/10.14295/bjs.v3i11.658

Fujimoto, H., Ando, Y., Yamashita, T., Terazaki, H., Tanaka, Y., Sasaki, J., & Ando, M. (1997). Nitric oxide synthase activity in human lung cancer. *Japanese Journal of Cancer Resea*rch, 88(12), 1190-1198. https://doi.org/10.1111/j.1349-7006.1997.tb00348.x

Gao, Y., Zhou, S., Xu, Y., Sheng, S., Qian, S. Y., & Huo, X. (2019). Nitric oxide synthase inhibitors 1400W and L-NIO inhibit angiogenesis pathway of colorectal cancer. *Nitric Oxide*, 83, 33-39. https://doi.org/10.1016/j.niox.2018.12.008

Halgren. (1998). Merck molecular force field. I. Basis, form, scope, parametrization, and performance of MMFF94. *Journal of Computational Chemistry*, 17(5-6), 490-519.

Hazai, E., Kovács, S., Demkó, L., & Bikádi, Z. (2009). DockingServer: molecular docking calculations online. *Acta pharmaceutica Hungarica*, 79(1), 17-21.

Hecht, S., & Hatsukami, D. (2022). Smokeless tobacco and cigarette smoking: chemical mechanisms and cancer prevention. *Nature Reviews Cancer*, 22(3), 143-155.

Huang, F., & Yu, S. (2018). Esophageal cancer: risk factors, genetic association, and treatment. *Asian Journal Surgery*, 41(3), 210-215. https://doi.org/10.1016/j.asjsur.2016.10.005

Im, P., Yang, L., Kartsonaki, C., Chen, Y., Guo, Y., & Du, H. (2022). Alcohol metabolism genes and risks of site-specific cancers in Chinese adults: An 11-year prospective study. *International Journal of Cancer* 150(10),1627-39. https://doi.org/10.1002/ijc.33917

Kampa, M., Hatzoglou, A., Notas, G., Niniraki, M., Kouroumalis, E., & Castanas, E. (2001). Opioids are non-competitive inhibitors of nitric oxide synthase in T47D human breast cancer cells. *Cell Death & Differentiation*, 8(9), 943-952.

Khrapova, M. V., Khrapov, S. E., Chechushkov, A. V., Kozhin, P. M., Romakh, L. P., Serykh, A. E., & Menshchikova, E. B. (2023). The toxicity of a new monophenolic synthetic inducer of Keap1/Nrf2/ARE redox-sensitive signaling system in vitro and in vivo. *Cell and Tissue Biology*, 17(3), 299-305.

Kong, R., Yang, G., Xue, R., Liu, M., Wang, F., Hu, J., & Chang, S. (2020). COVID-19 Docking Server: a meta server for docking small molecules, peptides and antibodies against potential targets of COVID-19. *Bioinformatics*, 36(20), 5109-5111. https://doi.org/10.1093/bioinformatics/btaa645

Krishnamoorthy, P. K., Balaraman, A. D., Priyadharshini, A., Shanmugam, D. A., Muthukumaran, S., Kesavamurthy, A., & Revanasiddappa, P. D. (2023). Molecular docking and simulation binding analysis of boeravinone B with caspase-3 and EGFR of hepatocellular carcinoma. *Letters in Drug Design & Discovery*, 20(2), 238-244. https://doi.org/10.2174/1570180819666220805163725

Lazarus, E., & Bays, H. (2022). Cancer and obesity: an obesity medicine association (OMA) clinical practice statement (CPS). *Obesity Pill*, 3,100026. https://doi.org/10.1016/j.obpill.2022.100026

Lazarus, E., & Bays, H. (2022). Cancer and obesity: an obesity medicine association (OMA) clinical practice statement (CPS) 2022. *Obesity Pillarys*, 3, 100026. https://doi.org/10.1016/j.obpill.2022.100026

Lee, A., Yang, X., Tyrer, J., Gentry-Maharaj, A., Ryan, A., Mavadda, N., & Antoniou, A. Comprehensive epithelial tubo-ovarian cancer risk prediction model incorporating genetic and epidemiological risk factors. *Journal of Medical Genetics*, 2022; 59(7), 632-643.

Liu, C. Y., Wang, C. H., Chen, T. C., Lin, H. C., Yu, C. T., & Kuo, H. P. (1998). Increased level of exhaled nitric oxide and up-regulation of inducible nitric oxide synthase in patients with primary lung cancer. *British Journal of Cancer*, 78(4), 534-541.

Lohachova, K. O., Sviatenko, A. S., Kyrychenko, A., Ivanov, V. V., Langer, T., Kovalenko, S. M., & Kalugin, O. N. (2024). Computer-aided drug design of novel nirmatrelvir analogs inhibiting main protease of Coronavirus SARS-CoV-2. *Journal of Applied Pharmaceutical Science*, 14(5), 232-239. https://dx.doi.org/10.7324/JAPS.2024.158114

Loibl, S., Buck, A., Strank, C., von Minckwitz, G., Roller, M., Sinn, H. P., & Kaufmann, M. (2005). The role of early expression of inducible nitric oxide synthase in human breast cancer. *European Journal of Cancer*, 41(2), 265-271. https://doi.org/10.1016/j.ejca.2004.07.010

Loibl, S., Von Minckwitz, G., Weber, S., Sinn, H. P., Schini-Kerth, V. B., Lobysheva, I., & Kaufmann, M. (2002). Expression of endothelial and inducible nitric oxide synthase in benign and malignant lesions of the breast and measurement of nitric oxide using electron paramagnetic resonance spectroscopy. *Cancer*, 95(6), 1191-1198. https://doi.org/10.1002/cncr.10817

Minhas, R., Bansal, Y., & Bansal, G. (2020). Inducible nitric oxide synthase inhibitors: A comprehensive update. *Medicinal Research Reviews*, 40(3), 823-855. https://doi.org/10.1002/med.21636

Morris, M., Goodsell, D., Hallyday, R., Huey, R., hart, W., Belew, R., & Olson, A. (1998). Automated docking using a Lamarckian genetic algorithm and an empirical binding free energy function. *Journal of Computational Chemistry*, 19(14**)**, 1639-1662. https://doi.org/10.1002/(SICI)1096-987X(19981115)19:14%3C1639:AID-JCC 10%3E3.0.CO;2-B

O'Sullivan, D., Sutherland, R., Town, S., Chow, K., Fan, J., Forbes, N., & Brenner, D. (2022). Risk factors for early-onset colorectal cancer: a systematic review and meta-analysis. *Clinical Gastroenterology and Hepatology*, 20(6), 1229-1240. https://doi.org/10.1016/j.cgh.2021.01.037

Phua, Z., MacInnis, R., % Jayasekara, H. (2022). Cigarette smoking and risk of second primary cancer: a systematic review and meta-analysis. *Cancer Epidemiology*, 78, 102160. https://doi.org/10.1016/j.canep.2022.102160

Qing, X., Yin Lee, X., De Raeymaeker, J., RH Tame, J., YJ Zhang, K., De Maeyer, M., & RD Voet, A. (2014). Pharmacophore modeling: advances, limitations, and current utility in drug discovery. *Journal of Receptor, Ligand and Channel Research*, 81-92.

Saad, M., Mokrab, Y., Halabi, N., Shan, J, Razali R, Kunji K, & Chouchane L. Genetic predisposition to cancer across people of different ancestries in Qatar: A population-based, cohort study. *The Lancet Oncology*, 2022; 23(3), 341-352.

Schaller, D., Šribar, D., Noonan, T., Deng, L., Nguyen, T. N., Pach, S., & Wolber, G. (2020). Next generation 3D pharmacophore modeling. *Wiley Interdisciplinary Reviews: Computational Molecular Science*, 10(4), e1468. https://doi.org/10.1002/wcms.1468

Siegel, R., Miller, K., Fuchs, H., Jemal, A. (2022). Cancer statistics. *CA Cancer Journal for Clinicians*, 72(1), 7-33. https://doi.org/10.3322/caac.21708

Solis, F., & Wets, R. (1981). Minimization by Random Search Techniques. *Mathematics of Operations Research*, 6 (1**),** 19-30. https://doi.org/10.1287/moor.6.1.19

Sushko, I., Salmina, E., Potemkin, V. A., Poda, G., & Tetko, I. V. (2012). ToxAlerts: a web server of structural alerts for toxic chemicals and compounds with potential adverse reactions. *Journal of Chemical Information and Modeling*, 52(8), 2310-2316. https://doi.org/10.1021/ci300245q

Swan, J., Szabó, Z., Peters, J., Kummu, O., Kemppi, A., Rahtu-Korpela, L, Magga, J. (2024). Inhibition of activin receptor 2 signalling ameliorates metabolic dysfunction–associated steatotic liver disease in western diet/L-NAME induced cardiometabolic disease. *Biomedicine & Pharmacotherapy*, 175, 116683. https://doi.org/10.1016/j.biopha.2024.116683

Tu, K., Ma, T., Zhou, R., Xu, L., Fang, Y., & Zhang, C. (2022). Association between Dietary Fatty Acid Patterns and Colorectal Cancer Risk: A Large-Scale Case-Control Study in China. *Nutrients*, 14(20), 4375. https://doi.org/10.3390/nu14204375

Verdonk, M. L., Cole, J. C., Hartshorn, M. J., Murray, C. W., & Taylor, R. D. (2003). Improved protein–ligand docking using GOLD. *Proteins: Structure, Function, and Bioinformatics*, 52(4), 609-623. https://doi.org/10.1002/prot.10465

Wan, Y., Wu, K., Wang, L., Yin, K., & Song, M. (2022). Dietary fat and fatty acids in relation to risk of colorectal cancer. *European Journal of Nutrition*, 61(4), 1863-1873.

Wolber, G., & Kosara, R. (2006). Pharmacophores from macromolecular complexes with LigandScout. *Pharmacophores and pharmacophore searches*, 32, 131-150. https://doi.org/ 10.1002/3527609164

Wolber, G., & Langer, T. (2005). LigandScout: 3-D pharmacophores derived from protein-bound ligands and their use as virtual screening filters. *Journal of chemical information and modeling*, 45(1), 160-169. https://doi.org/10.1021/ci049885e

Xia, C., Dong, X., Li, H., Cao, M., Sun, D., He, S., & Chen, W. (2022). Cancer statistics in China and United States, 2022: profiles, trends, and determinants. *Chinese Medical Journal*, 135(5), 584-590.

Yagihashi, N., Kasajima, H., Sugai, S., Matsumoto, K., Ebina, Y., Morita, T., & Yagihashi, S. (2000). Increased in situ expression of nitric oxide synthase in human colorectal cancer. *Virchows Archiv*, 436, 109-114.

Yang, S. Y. (2010). Pharmacophore modeling and applications in drug discovery: challenges and recent advances. *Drug Discovery Today*, 15(11-12), 444-450. https://doi.org/10.1016/j.drudis.2010.03.013

Yoo, J., Han, K., Shin, D., Kim, D., Kim, B., & Chun, S. (2022). Association Between Changes in Alcohol Consumption and Cancer Risk. *Journal of American Medical Association*, 5(8), e2228544. https://doi.org/10.1001/jamanetworkopen.2022.28544

Funding

Not applicable.

Intitutional Review Board Statement

Not applicable.

Informed Consent Statement

Not applicable.